Indian Journal of Experimental Biology
Vol. 64, August 2026, pp.701-709
DOI: 10.56042/ijeb.v64i08.26787

Human bone marrow mesenchymal stem cell–derived extracellular vesicles enriched with miR-146a attenuate myocardial ischemia–reperfusion injury via suppression of inflammatory and oxidative stress pathways

Daming Mu[1], Yang Liu[1], Zhichao Zhang[1], Yue Shang[1], Yinghui Wang[1] & Zhanxiu Zhang[2]*

[1]Department of Cardiology, Huludao Second People's Hospital, Huludao City, L iaoning Province, 125001, China

[2]Heart Center, Huludao Second People's Hospital, Huludao City, Liaoning Province, 125001, China

Received 31 December 2025; revised 15 March 2026

This study aims to evaluate the cardioprotective properties of miR-146a-enriched Extracellular vesicles (EV) derived from human bone-marrow mesenchymal stem cells (MSCs) (BMSCs). BMSCs were transfected with miR-146a mimics or control mimics, and the EVs were isolated. Thirty Sprague-Dawley male rats were randomly divided into myocardial I/R Control, I/R + EV control, and I/R + miR-146a EVs groups, and EVs were administered intravenously at the time of reperfusion. Afterward, plasma cardiac troponin I (cTnI), creatine kinase-MB (CK-MB), malondialdehyde (MDA), superoxide dismutase (SOD), glutathione peroxidase (GSH-Px), TNF-α, IL-6, and IL-1β were measured using ELISA, and IRAK1, TRAF6, NF-κB1, NLRP3, Caspase 1, IL-1β, Nox2, and Nox4 were evaluated in left ventricular tissue by RT-PCR. Results indicated that the miR-146a-enriched EVs reduced plasma levels of cTnI, CK-MB, and MDA, and increased plasma levels of SOD and GSH-Px compared with the control groups. Levels of TNF-α, IL-6, and IL-1β were also significantly reduced. RT-qPCR further showed that TRAF6 and NF-κB1 were downregulated, with decreased transcription of NLRP3, Caspase 1, IL-1β, and oxidative stress markers Nox2 and Nox4. MSC-derived EVs enriched with miR-146a can reduce myocardial I/R injury in rats by inhibiting inflammatory and oxidative-stress pathways via inhibition of the TRAF6/NF-κB/NLRP3 axis.

Keywords: miRNA, immunomodulation, bone-marrow, inflammation, Mesenchymal Stem Cell

Introduction

One of the main obstacles to treating myocardial infarction (MI) is myocardial ischemia-reperfusion injury (MIRI), which is the paradoxical injury to heart tissue that develops after blood flow is restored following an MI event[1]. The mechanism by which reperfusion injury occurs involves several different factors that need to work together in order for the injury to occur. Oxidative stress, inflammatory response, calcium overload, mitochondrial dysfunction, and damage to cardiac muscle cells caused by either necrosis (cell death) or pyroptosis (cell death due to inflammation) all play a role in the mechanism of injury[2,3]. Of these factors, inflammatory response and oxidative stress can be considered the two main contributors to the development of reperfusion injury. Following restoration of blood supply, oxygen is reintroduced, and as a result, an increase in the formation of reactive oxygen species (ROS) occurs, leading to lipid peroxidation, opening of the mitochondrial permeability transition pore, and cell death[4]. In addition, the activation of intracellular inflammatory signaling pathways occurs at the same time through the action of pattern recognition receptors present on both immune and cardiovascular cells[5].

Mesenchymal stem cells (MSCs) have gained traction over the previous decade as a viable approach to repairing the heart, not solely based on new MSC usage in engraftment, but due largely to their paracrine effects[6,7]. This change in perspective has led to increased interest and research on extracellular vesicles derived from MSCs (MSC-EVs), including exosomes and microvesicles, which can transfer bioactive next proteins, lipids, and nucleic acids to damaged cells[8]. Furthermore, compared to using MSCs directly, EVs have many advantages, including less immunogenicity, no ability to form tumors, more stability in storage conditions, and more readily available and feasible to manufacture and modify in large quantities[9]. Preclinical studies have demonstrated that EVs derived from MSCs have potent cytoprotective, anti-inflammatory, and antioxidant properties when placed into animal

*Correspondence:
E-mail: zzx15542906555@outlook.com

models of cardiac injury[10]. The therapeutic actions of these EVs are heavily influenced by the miRNA cargos contained within the EVs[11].

Of the many miRNAs involved in cardiovascular protection, miR-146a has been identified as an important miRNA of the innate immune response[12]. MiR-146a regulates the activity of TRAF6 and IRAK1, which are essential adapters in the signaling cascade leading to NF-κB activation and production of pro-inflammatory cytokines[13,14]. Although miR-146a's role in the treatment of myocardial injury has not yet been comprehensively investigated, prior data indicate its importance as a miRNA; however, miR-146a has been identified as a critical modulator of inflammation and oxidative stress, which are two major contributors to reperfusion injury and may therefore serve as a candidate for enhancing the therapeutic efficacy of EVs. This study is the first to directly compare the cardioprotective efficacy of miR-146a-enriched EVs derived from human bone marrow-derived MSCs with that of non-modified equivalent EVs in a rat model, thereby elucidating the added therapeutic value of targeted miRNA enrichment in EV-based cardiac repair.

Materials and Methods

Isolation and characterization of BMSCs

Bone marrow aspirates from anonymous sources, with informed consent and in conformity with the Declaration of Helsinki, were used in this study. Mononuclear cells were separated from the aspirates using a procedure called Ficoll density gradients. In the process of creating mononuclear cell samples, a diluted sample of bone marrow was layered onto a Ficoll layer and centrifuged at 400 x g for 30 minutes. The top layer of mononuclear cells was collected and washed with PBS before being suspended in MSC media. Cells were plated in tissue culture dishes at 2 × 10^6 cells per well and maintained in MSC basal medium containing 10% human platelet lysate, 1% L-glutamine, and 1% penicillin–streptomycin. After 24 hours, the culture media were changed to remove all non-adherent mononuclear cells. Adherent MSCs were grown at a temperature of 37 °C and a CO2 level of 5%; the culture medium was switched every 2-3 days. At a point in time where the cultures were approximately 85-90% confluent, MSCs were detached from the substratum by using trypsin/EDTA, diluted with the appropriate media, and then cryopreserved. MSCs grown at passages of 3-5 after primary isolation were subjected to experimentation. Characterization of BMSCs from passages 3-5 was performed to establish their identity. Flow cytometric analysis for positive expression of CD44 and CD90, and negative expression of CD45, was done to confirm that they are indeed BMSCs. Assessment of the multilineage differentiation potential, which is one of the major characteristics of stem cells, was made by inducing osteogenic and adipogenic differentiation.

BMSCs transfection with miR-146a

To carry out the transfection procedure, BMSCs were grown to an approximate 80% confluency before transfecting them with the Lipofectamine 3000 reagent (Thermo Fisher Scientific) in the Opti-MEM medium for 3 days (72 hours). As per the manufacturer's instructions, the miRNA-146a (miR-146a) mimics and their controls (mimic NC) were used at a ratio of 1:100 mimics to the reagents.

EV isolation and characterization

EVs from BMSCs transfected with either a miR-146a mimic or a control mimic were obtained from the medium of the cells at a confluency of 85-90%. The media in which the cells were grown were replaced with fresh media containing fetal bovine serum (FBS) that had been depleted of EVs. The EV-depleted FBS was prepared by centrifuging at 500 × g for 20 minutes; then by centrifuging again at 20,000 × g for 30 minutes; and finally ultracentrifuging at 110,000 × g for 7 hours at 4°C, and filtering (0.22 μm) the supernatant. The conditioned media were collected at 48 hours post-change and centrifuged differentially:

(1) 500 × g for 20 minutes.
(2) 20,000 × g for 30 minutes.

After each stage of centrifugation, the pellets were removed and the supernatant centrifuged again twice at 110,000 × g for 70 minutes to obtain a pellet of EVs. The final pellet of EVs was resuspended in 1 mL of sterile phosphate-buffered saline. The BMSC-EV size distribution and average size of BMSC-EVs were further determined using a HORIBA SZ-100 at a 173° scatter angle with a 30% ND filter. Sample fluidization took place using PBS, and BMSC-EVs were analyzed at 25.2°C. Data were processed using the HORIBA software (version 2.20). Protein concentrations were determined using the Protein Bicinchoninic Acid (BCA) Assay Kit (Solarbio, China).

Animals and experimental myocardial ischemia–reperfusion model

Thirty adult male Sprague-Dawley rats weighing between 180-200 g were housed in a standard laboratory environment (12-hour dark-light cycle with access to food and water). All experimental protocols were approved by the Huludao Second People's Hospital (Ethical No: (2024) Annual Review No. (09)). To induce an ischemia-reperfusion (I/R) injury model, we performed left anterior descending (LAD) coronary artery ligation as previously described[15] but modified to accommodate a rat surgery technique. Briefly, rats were anesthetized with pentobarbital sodium (50 mg/kg, intraperitoneally), intubated, and placed on mechanical ventilation. A left thoracotomy was performed at the fourth intercostal space to gain access to the heart. The LAD artery was ligated approximately 2-3 mm distal from the tip of the left atrial appendage with a 6-0 silk suture with protective polyethylene tubing. Ischemia was confirmed by visual observation of a regional whitish color change due to inadequate blood flow. Ischemic status was maintained for 30 minutes. After this period, reperfusion was initiated after the knot was untied and confirmed by returning colors and movement to the myocardium. Animals were distributed randomly into one of three groups (I/R Control received PBS; I/R with control EVs; or I/R with miR-146a-enriched EVs) before initiation of the study. All treatment animals received tail vein injections of 100 μg of EVs suspended in sterile PBS at the onset of reperfusion. Blood samples were collected from the abdominal aorta to determine plasma levels at the scheduled endpoints, while left ventricular tissue was utilized for future molecular analyses. Any animal with intraoperative complications severe enough to result in death (e.g., uncontrolled hemorrhage or fatal arrhythmias) was removed from the trial.

Splenocyte isolation and culture

This study assessed splenocyte material to support cytokine analysis. Spleens were aseptically removed from rats at the time of sacrifice, and each spleen was placed in a single-cell solution using a 70 μm filter. RBCs in the solution were removed with a commercial buffer solution for RBC lysis. Following RBC lysis, purified splenocyte cells were cultured using RPMI-1640 growth medium with the addition of 10% FBS (thereafter named splenocyte growth medium) and 1% penicillin/streptomycin antibiotic solution.

Biochemical markers and cytokines assay

Specific ELISA tests and controls were performed on both splenocyte culture supernatant fluids and plasma samples, using commercial sandwich ELISA kits (cTnI: ab246529, Abcam, USA, CK-MB: ab285275, Abcam, USA, MDA: A247177, Antibodies, UK, SOD: A80164, Antibodies, UK, GSH-Px: MBS3807927, MyBioSource, USA) in accordance with the manufacturer's instructions, for the identification of specific biomarkers.

Plasma was collected for testing for cardiac damage by measuring the levels of cTnI and CK-MB, as well as oxidative stress markers (MDA, SOD, and GSH-Px).

To assess the inflammatory response, supernatants from splenocyte cultures were tested for the presence of pro-inflammatory cytokines (TNF-α, IL-6, and IL-1β).

Real-Time PCR analysis of gene expression in left-ventricular tissues

We isolated total RNA from left ventricular tissue samples taken from all experimental test groups. The left ventricular tissue was processed using TRIzol reagent. The total RNA was obtained in accordance with the instructions outlined by the manufacturer. We evaluated the concentration and purity of the total RNA extracted from left ventricle samples with a NanoDrop spectrophotometer.

To analyze the expression of specific mRNA, we reverse transcribed 1 μg of total RNA into complementary DNA (cDNA) using the High-Capacity cDNA Reverse Transcription Kit (Applied Biosystems) following the manufacturer's specifications.

Real-time PCR was used to evaluate the expression of inflammation, inflammasome activation, and oxidative stress-related genes; specifically, TRAF6 and NFκB1 (p105) as primary inflammatory signaling mediators; NLRP3 and Caspase-1 as early components of the inflammasome; IL-1β as the downstream effector of the inflammasome; and Nox2 and Nox4 as oxidative stress markers.

For all PCR reactions, the total mixture was 20 μL, consisting of 10 μL of SYBR Green Master Mix (Applied Biosystems), 1 μL of cDNA template, and each specific forward and reverse primer was included at 0.5 μM concentration. Amplifications were performed in the ABI 7500 Real-Time PCR system under the following conditions: an initial denaturation step at 95°C for 10 minutes, followed by denaturation at 95°C for 15 seconds and a combined

annealing/extension at 60°C for 1 minute for 40 cycles total. A melting curve analysis was performed on the PCR products to verify the specificity of the amplified products. The resultant relative expression level of all target genes was normalized against the expression level of the housekeeping gene GAPDH, and the expression levels of all target genes were determined using the $2^{-\Delta\Delta Ct}$ method.

Statistical analysis

Descriptive statistical analyses were performed using IBM SPSS Statistics (version 26). The data are presented as means ± standard deviation. A p-value of less than 0.05 is considered statistically significant. The normal distribution of the data was tested using the Shapiro-Wilk test. For normally distributed data, group comparisons were made using one-way analysis of variance (ANOVA) with Tukey's post hoc test. For non-normally distributed data, Kruskal-Wallis was used to compare groups. Data were presented graphically using GraphPad Prism (version 8).

Results

BMSCs characterization

During both the initial and re-passage stages of primary culture, BMSCs obtained from the bone marrow displayed the typical spindle-shaped fibroblast-like appearance of MSC when examined individually (Fig. 1a). Upon an examination of a population of isolated BMSCs, it became evident that they reached approximately 70%-80% confluence after 5 to 7 days,

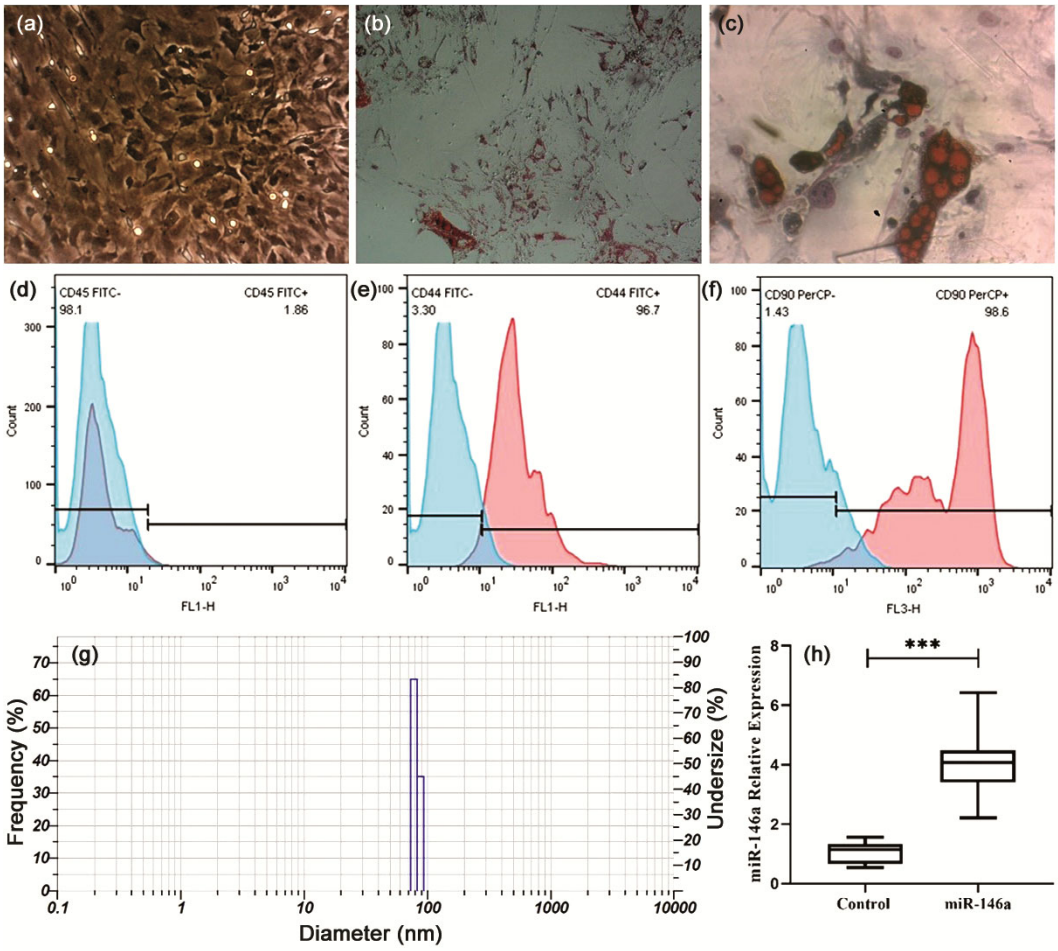

Fig. 1 — Characterization of Human Bone Marrow–Derived Mesenchymal Stem Cells (BMSCs) and Their Extracellular Vesicles (EVs). (a) Representative morphology of cultured BMSCs showing a spindle-shaped, fibroblast-like appearance. (b) Osteogenic differentiation confirmed by Alizarin Red staining, demonstrating calcified nodule formation. (c) Adipogenic differentiation confirmed by Oil Red O staining, showing intracellular lipid droplets. (d–f) Flow cytometric analysis showing high expression of MSC markers CD44 and CD90 and low expression of hematopoietic marker CD45. (g) DLS confirmation of EV diameter in isolated BMSC-EVs. (h) Relative miR-146a expression levels in EVs derived from BMSCs transfected with miR-146a mimics vs. control mimics. BMSC-EV, bone marrow-derived mesenchymal stem cell-extracellular vesicle. DLS, dynamic light scattering.

which fits into the MSC growth pattern prediction. The multilineage differentiation capability of the cultured BMSCs was confirmed after alkaline phosphatase induction was achieved. Following this, good deposition of calcified nodules was visible via Alizarin Red staining, thereby confirming successful osteogenic differentiation (Fig. 1b). The deposition of large numbers of intracellular lipid droplets in BMSCs treated under adipogenic differentiation conditions was identified using Oil Red-O staining, indicating efficient and complete differentiation into adipose tissue (Fig. 1c).

Moreover, it was determined through flow cytometry that the identity of cultured cells matched the BMSC phenotype. The isolated cells were negative for the hematopoietic marker CD45 (Fig. 1d) but exhibited high surface expression of the MSC markers CD44 (Fig. 1e) and CD90 (Fig. 1f), confirming a highly pure BMSC population.

Collectively, the results from these experiments confirm that the BMSCs, which were isolated and expanded, are both functionally and biologically consistent with those observed from BMSCs that possess the biological characteristics of MSCs.

The BMSC-EVs Characterization

The hydrodynamic size dispersion of the BMSC-EVs was determined using DLS. The EV preparation displayed a monomodal, narrow size distribution that indicates homogeneity within the isolated population of MSC-EVs. The highest peak of the distribution was at approximately 80-100 nm, in the range of expected size for small EVs. The frequency plot supported this by demonstrating that >80% of the EVs were represented within this peak, thus confirming the homogeneity and quality of the isolation process. These findings indicate that isolated BMSCs are primarily composed of nanoscale EVs appropriate for the following biological assays (Fig. 1g).

Encapsulation of miR-146a in BMSCs

When we evaluated the amount of miRNA found in the EVs, we found that BMSCs transfected with miR-146a produced high levels of miR-146a in the EVs compared to control EVs. This finding provides evidence that BMSCs have the capability to load miRNA into EVs (Fig. 1h). This finding also indicates that BMSC transfection was successful in modifying the molecular content of the resulting EVs while having no effect on their general structural morphology.

ELISA analysis of cardiac injury, oxidative stress, and inflammatory markers

ELISA measurements indicated that there were significant differences in the myocardial injury and systemic inflammation among the experimental groups. After administering EVs with miR-146a, levels of cTnI and CK-MB were significantly decreased compared to the control PBS (P <0.0001) and control EV groups (P=0.0001and P<0.0001, respectively) (Fig. 2). Therefore, we conclude that the degree of cardiomyocyte injury was reduced after treatment with EVs containing miR-146a.

The markers of oxidative stress also displayed a treatment-dependent effect. Specifically, I/R injury increased lipid peroxidation, as indicated by elevated MDA levels, while simultaneously decreasing the antioxidant activity of both SOD and GSH-Px. Following treatment with miR-146a-EVs, levels of MDA were significantly reduced (P<0.0001 compared to the control PBS and P= 0.0013 compared to control EV), along with the restoration of SOD and GSH-Px activity when compared to the control PBS (P<0.0001) and control EV groups (P=0.0009 and P=0.0102, respectively), indicating improved redox status and reduced oxidative stress (Fig. 3).

To measure the inflammatory response, we evaluated the concentration of cytokines present in splenocyte supernatants. Large amounts of TNF-α, IL-6, and IL-1β were measured in splenocyte supernatants following I/R injury, demonstrating

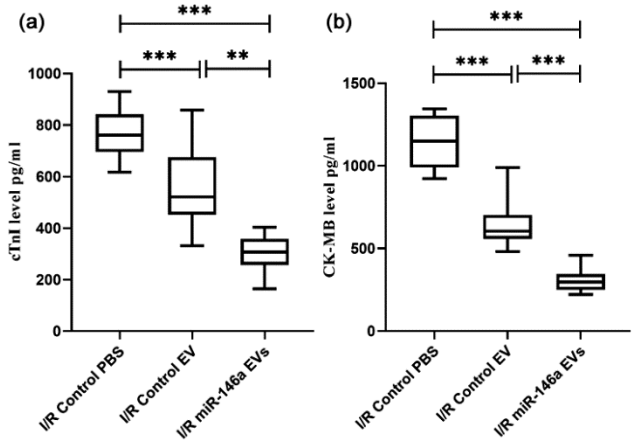

Fig. 2 — Plasma Cardiac Injury Markers Following Myocardial Ischemia–Reperfusion (I/R) Injury and EV Treatment. Plasma levels of cardiac troponin I (cTnI) and creatine kinase-MB (CK-MB) in the PBS control, control EV, and miR-146a-EV groups. miR-146a-EV treatment significantly reduced myocardial injury biomarkers compared with controls. Data shown as mean ± SD. N=10/group. (*P < 0.05, ** P < 0.01, *** P < 0.001).

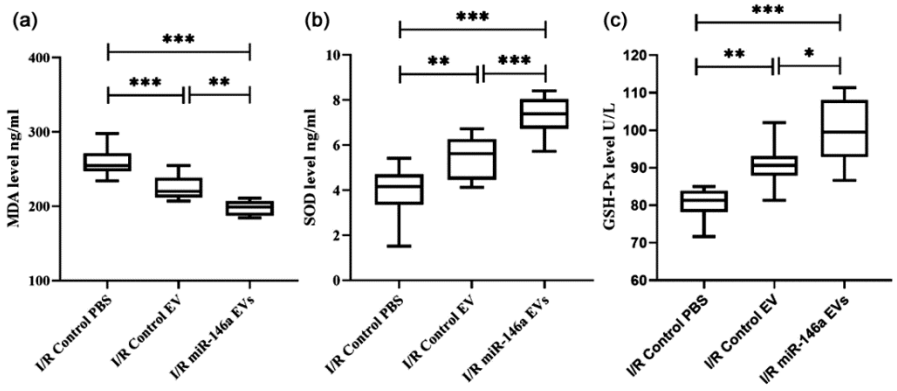

Fig. 3 — Oxidative Stress Marker Levels in Plasma After Myocardial I/R and EV Treatment. Levels of malondialdehyde (MDA), superoxide dismutase (SOD), and glutathione peroxidase (GSH-Px) in each treatment group. miR-146a-EVs significantly decreased MDA and restored antioxidant enzyme activity compared with controls. Data shown as mean ± SD. N=10/group. (*$P < 0.05$, ** $P < 0.01$, *** $P < 0.001$).

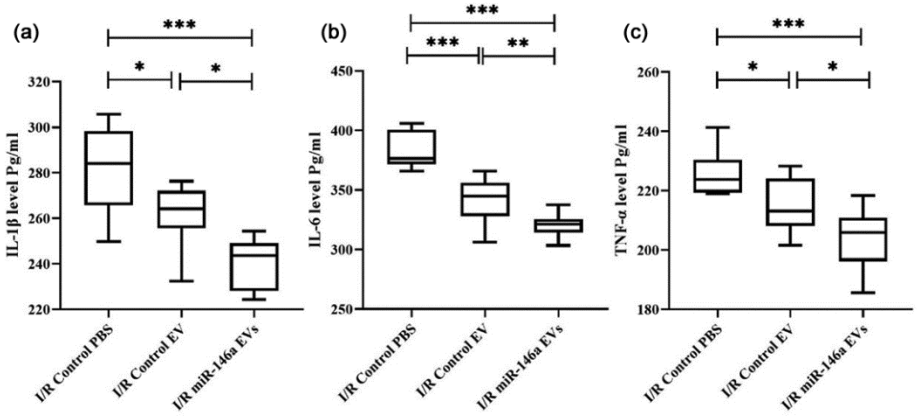

Fig. 4 — Inflammatory Cytokine Production in Splenocyte Supernatants Following I/R Injury and EV Treatment. Concentrations of TNF-α, IL-6, and IL-1β measured by ELISA. Treatment with miR-146a-EVs significantly reduced systemic inflammatory cytokine release compared with PBS and control EV groups. Data shown as mean ± SD. N=10/group. (*$P < 0.05$, ** $P < 0.01$, *** $P < 0.001$).

robust inflammatory signaling at the level of systemic inflammation. Treatment with miR-146a-EVs resulted in significant reductions in TNF-α, IL-6, and IL-1β levels compared to both the PBS control (I/R Control) ($p<0.0001$)and the control EV groups ($p=0.0279$, 0.0092, 0.0127, respectively), indicating that the anti-inflammatory activity was mediated by the EV containing miR-146a (Fig. 4).

Taken together, these ELISA results demonstrate that miR-146a-enriched BMSC-EVs effectively mitigate myocardial injury, reduce oxidative stress, and suppress inflammatory cytokine production following I/R injury, confirming their multifaceted protective role.

Expression of miR-146a and Its Canonical Targets

Our results showed that the mRNA expression levels of IRAK1, TRAF6, and NF-κB1 (p105), the downstream targets of miR-146a, were significantly decreased in the miR-146a group when compared to those of the control PBS ($P<0.0001$) and control EV group *(*$P=0.0034$, 0.0211, respectively), illustrating the inhibition of the NF-κB signaling pathway (Fig. 5).

Inflammasome-Related Gene Expression

MiR-146a-EV treatment significantly decreased the component genes of the inflammasome (NLRP3, Caspase-1) through a significant decrease in their mRNA levels when comparing the miR-146a-EV group with the control PBS *(*$P<0.0001$) and control EV groups ($P= 0.0110$ and $P= 0.0098$, respectively) (Fig. 6). This result parallels the decrease in mRNA production of the downstream inflammatory mediator IL-1β as a result of decreased activation of the inflammasome ($P<0.0001$ compared to the control

PBS and *P*=0.0329 compared to the control EV group).

Oxidative stress markers

NADPH Oxidase (Nox2 and Nox4), as the major mediators of oxidative stress produced by the cell, were also significantly decreased in the miR-146a-EV group when compared to the control PBS (*P*<0.0001) and control EV group (*P*=0.0459 and p=0.0216, respectively) (Fig. 7). This result is consistent with the decreased levels of the oxidative stress markers as they were determined by ELISA, and provides support for the hypothesis that miR-146a mediates a transcriptional reduction of oxidative stress.

Discussion

This study shows that the therapeutic effects of MSC-EVs are augmented by the addition of miR-146a, which effectively reduces myocardial reperfusion injury by reducing inflammation and oxidative stress. These data add to the growing body of literature that supports a critical role for EV-mediated RNA transfer as a mechanism of action for the cardiac repair capabilities attributed to MSC-EVs, as previously published[16, 17]. The current study expands upon this work by identifying miR-146a enrichment within EVs as a means of expanding their therapeutic capability.

One of the key findings of this study was that plasma levels of cardiac troponin I and CK-MB were significantly decreased as a result of administering mir-146a-EVs. The reduction in biomarkers demonstrates that miR-146a-EVs reduce cardiomyocyte damage from reperfusion and, therefore, support cardiomyocyte

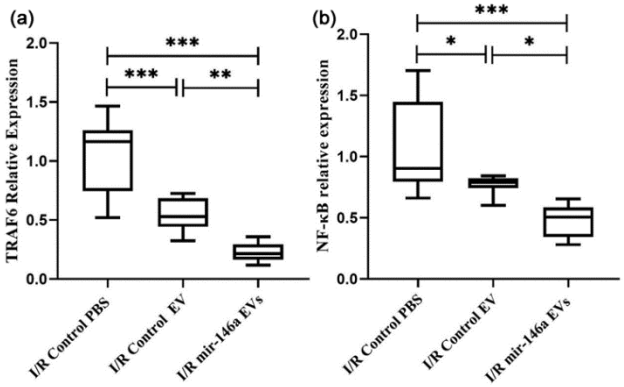

Fig. 5 — Expression of miR-146a Target Genes IRAK1, TRAF6, and NF-κB1 in Left Ventricular Tissue. Relative mRNA levels of IRAK1, TRAF6, and NF-κB1 (p105) analyzed by RT-qPCR. miR-146a-EV treatment significantly downregulated these genes, indicating suppression of NF-κB signaling. Data shown as mean ± SD. N=10/group. (*$P < 0.05$, ** $P < 0.01$, *** $P < 0.001$).

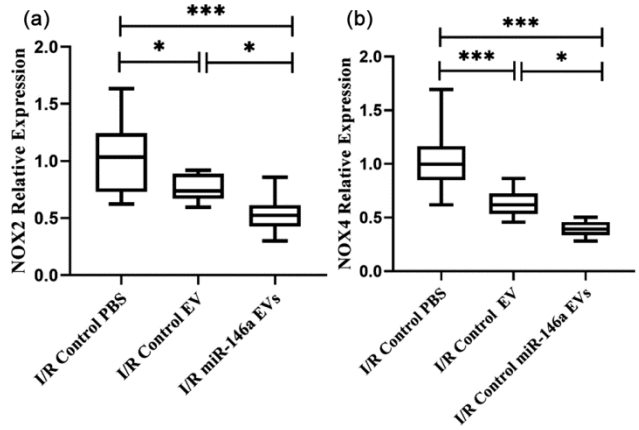

Fig. 7 — Oxidative stress-related gene expression in left ventricular tissue following treatment. Relative expression of NADPH oxidase isoforms Nox2 and Nox4. miR-146a-EV treatment significantly decreased transcription of both oxidative stress mediators. Data shown as mean ± SD. N=10/group. (*$P < 0.05$, ** $P < 0.01$, *** $P < 0.001$).

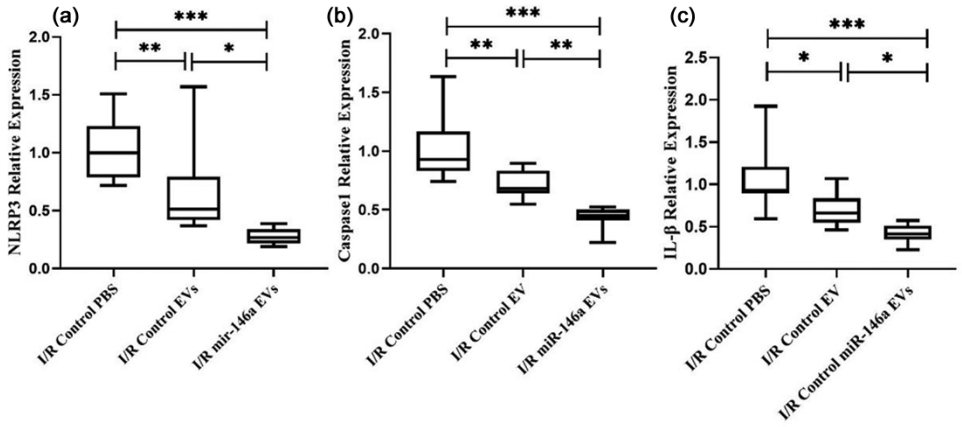

Fig. 6 — Inflammasome-related gene expression in left ventricular tissue after treatment. RT-qPCR quantification of NLRP3, Caspase-1, and IL-1β mRNA levels. miR-146a-EVs significantly reduced the expression of inflammasome components compared with control groups. Data shown as mean ± SD. N=10/group. (*$P < 0.05$, ** $P < 0.01$, *** $P < 0.001$).

survival through the delivery of active biological materials to the cells. The finding corroborates previous studies that show that MSC-EVs also exhibit cardioprotective qualities by reducing apoptosis, oxidative stress, and inflammation[18,19]. The current study advances the understanding of this mechanism, as it demonstrates that by increasing the expression of miR-146a in EVs, the cardioprotective effects of MSC-EVs can be further enhanced.

A clear correlation between the reduction of pro-inflammatory cytokines due to miR-146a delivery and the biological functions of miR-146a has been established. miR-146a is recognized for its role in the negative regulation of TLR and cytokine signaling through TRAF6 and IRAK1 downregulation, which helps limit downstream activation of NF-κB[20, 21]. Reperfusion-mediated injury in cases such as a heart attack is due to the production of TNF-α, IL-6, and IL-1β, which are activated by NF-κB[5]. The marked decrease in systemic production of inflammatory cytokines observed in this study indicates that miR-146a was successfully delivered and that the inflammatory cascade has been inhibited. Similar observations were made using EVs containing miR-146a in colitis and ocular inflammation models, showing that miR-146a-containing EVs inhibited TRAF6 and IRAK1 expression and reduced the levels of inflammatory cytokines[13, 14].

In addition to its role in mediating inflammatory processes, this manuscript also provides an additional component for understanding how miR-146a interacts with oxidative stress and other mechanisms that result in ischemia/reperfusion injury. ROS that are produced during reperfusion lead to impaired mitochondrial function, increased levels of lipid peroxidation, and eventual death of cardiomyocytes [2]. The increase in antioxidant enzyme activity (SOD and GSH-Px) and the decrease in malondialdehyde levels observed in the miR-146a–EV-treated group support the possibility that miR-146a may have a role in the regulation of oxidative stress by inhibiting the expression of NF-κB-dependent NADPH oxidase isoforms, including Nox2 and Nox4, which is supported by previous findings regarding the role of NF-κB in regulating Nox expression following oxidative stress[22].

The demonstration that miR-146a–EVs have the ability to inhibit the activation of the inflammasome by NLRP3 represents another major contribution of the research. The NLRP3 inflammasome is responsible for the activation of Caspase-1 and IL-1β maturation, and is one of the main mediators of pyroptotic cell death induced by engraftment (I/R) in mice[23]. Thus, miR-146a–EVs are likely to attenuate both the expression of NLRP3 and Caspase-1 and to inhibit this additional layer of inflammatory injury. There is also evidence that NF-κB functions as a 'priming' signal for NLRP3, providing an additional mechanism to explain why there were reductions in NLRP3 and Caspase-1 mRNA levels following treatment with miR-146a–EVs[24]. Therefore, miR-146a is likely to be a 'multi-target' therapeutic for the modulation of both cytokine signaling and cell death pathways.

In addition, this research showed that miR-146a can be successfully added to EVs with no change to their existing identity or morphology, which represents a significant translational advancement. Engineered MSC-EVs may be used as a promising alternative to MSC transplantation because EVs do not have many of the safety issues related to stem cells; that is, EVs do not cause immunogenicity, do not lead to tumor formation, and have a higher level of stability in vivo, while still producing biological repair effects[8]. Furthermore, the ability to concentrate specific miRNAs in EVs could allow for the development of EV therapeutics that are optimized for certain disease-specific molecular pathways.

Several limitations of this study must be acknowledged. This study utilizes a short-term reperfusion model (for 2 hours), which reflects the early inflammatory and oxidative mechanisms of reperfusion injury; therefore, it does not investigate the chronic repair or the functional healing of the heart. A long-term assessment (e.g., echocardiographic assessment of the ventricular function) is necessary to determine if the molecular changes observed in the current study yield functional improvements within the heart after a longer period of time following myocardial I/R injury. Additionally, while rodent studies provide valuable mechanistic understanding of the process, there is a significant degree of caution regarding any translation to human beings because of the differences in immune responses between species, myocardial biology, and the pharmacokinetic properties of EVs.

Conclusion

In conclusion, the data presented in the current study provide strong evidence that engineered MSC-EVs, containing miR-146a, can significantly improve I/R injury and provide protective effects by

modulating prominent pathways associated with inflammation and oxidative stress. Thus, we propose that miR-146a could act as a promising therapeutic target to enhance the treatment and healing of the heart after myocardial infarction and support the future viability of engineered EVs for cardiac tissue repair. Future work to expand on these findings using long-term and large-animal models will likely facilitate the eventual clinical translation of this approach into the care of patients suffering from myocardial infarction.

Ethics Approval and Consent to Participate

All experimental protocols were approved by the Huludao Second People's Hospital (Ethical No.: (2024) Annual Review No. (09)). All methods were carried out in accordance with relevant guidelines and regulations, including the Declaration of Helsinki. Written informed consent was obtained from all participants before their enrollment in the study.

Conflict of Interest

The author declares no conflicts of interest.

References

1 Sagris M, Apostolos A, Theofilis P, Ktenopoulos N, Katsaros O, Tsalamandris S, Tsioufis K, Toutouzas K & Tousoulis D. Myocardial Ischemia–Reperfusion injury: Unraveling pathophysiology, clinical manifestations, and emerging prevention strategies. *Biomedicines*.12 (2024) 802.

2 Turer AT & Hill JA. Pathogenesis of myocardial ischemia-reperfusion injury and rationale for therapy. *Am J Cardiol*. 106 (2010) 360.

3 Hausenloy DJ & Yellon DM. Myocardial ischemia-reperfusion injury: a neglected therapeutic target. *J Clin Invest*. 123 (2013) 92.

4 Murphy E & Steenbergen C. Mechanisms underlying acute protection from cardiac ischemia-reperfusion injury. *Physiol rev*. 88 (2008) 581.

5 Frangogiannis NG. Pathophysiology of myocardial infarction. *Compr Physiol*. 5 (2015) 1841.

6 Burchfield JS & Dimmeler S. Role of paracrine factors in stem and progenitor cell mediated cardiac repair and tissue fibrosis. *Fibrogenesis & tissue repair*. 1 (2008) 4.

7 Mirotsou M, Jayawardena TM, Schmeckpeper J, Gnecchi M & Dzau VJ. Paracrine mechanisms of stem cell reparative and regenerative actions in the heart. *J Mol Cell Cardiol*. 50 (2011) 280.

8 Rani S, Ryan AE, Griffin MD & Ritter T. Mesenchymal stem cell-derived extracellular vesicles: toward cell-free therapeutic applications. *Mol ther*. 23 (2015) 812.

9 Flamant S, Loinard C & Tamarat R. MSC beneficial effects and limitations, and MSC-derived extracellular vesicles as a new cell-free therapy for tissue regeneration in irradiated condition. *Environ Adv*. 13 (2023) 100408.

10 Qin D, Wang X, Pu J & Hu H. Cardiac cells and mesenchymal stem cells derived extracellular vesicles: a potential therapeutic strategy for myocardial infarction. *Front Cardiovas Med*. 11 (2024) 1493290.

11 Ragni E, Banfi F, Barilani M, Cherubini A, Parazzi V, Larghi P, Dolo V, Bollati V & Lazzari L. Extracellular vesicle-shuttled mRNA in mesenchymal stem cell communication. *Stem cells*. 35 (2017) 1093.

12 Arroyo AB, Águila S, Fernández-Pérez MP, de Los Reyes-García AM, Reguilón-Gallego L, Zapata-Martínez L, Vicente V, Martínez C & González-Conejero R. miR-146a in cardiovascular diseases and sepsis: an additional burden in the inflammatory balance? *Thromb Haemost*. 121 (2021) 1138.

13 Wu H, Fan H, Shou Z, Xu M, Chen Q, Ai C, Dong Y, Liu Y, Nan Z & Wang Y. Extracellular vesicles containing miR-146a attenuate experimental colitis by targeting TRAF6 and IRAK1. *Int immunopharmacol*. 68 (2019) 204.

14 Han R, Gao J, Wang L, Hao P, Chen X, Wang Y, Jiang Z, Jiang L, Wang T & Zhu L. MicroRNA-146a negatively regulates inflammation via the IRAK1/TRAF6/NF-κB signaling pathway in dry eye. *Sci Rep*. 13 (2023) 11192.

15 Gao E & Koch WJ. A novel and efficient model of coronary artery ligation in the mouse. *Methods Mol Biol*. 1037 (2013) 299.

16 Bollini S, Smits AM, Balbi C, Lazzarini E & Ameri P. Triggering endogenous cardiac repair and regeneration via extracellular vesicle-mediated communication. *Front physiol*. 9 (2018) 1497.

17 Porada M, Janas A & Bajdak-Rusinek K. Extracellular vesicles in cardiac regeneration and aging: mechanisms and translation. *J Cardiovasc Aging*. 5 (2025) 19.

18 Arslan F, Lai RC, Smeets MB, Akeroyd L, Choo A, Aguor EN, Timmers L, van Rijen HV, Doevendans PA & Pasterkamp G. Mesenchymal stem cell-derived exosomes increase ATP levels, decrease oxidative stress and activate PI3K/Akt pathway to enhance myocardial viability and prevent adverse remodeling after myocardial ischemia/reperfusion injury. *Stem cell research*. 10 (2013) 301.

19 Lai RC, Arslan F, Lee MM, Sze NSK, Choo A, Chen TS, Salto-Tellez M, Timmers L, Lee CN & El Oakley RM. Exosome secreted by MSC reduces myocardial ischemia/reperfusion injury. *Stem cell research*. 4 (2010) 214.

20 Taganov KD, Boldin MP, Chang KJ & Baltimore D. NF-κB-dependent induction of microRNA miR-146, an inhibitor targeted to signaling proteins of innate immune responses. *Proc Natl Acad Sci U S A*. 103 (2006) 12481.

21 Jiang W, Kong L, Ni Q, Lu Y, Ding W, Liu G, Pu L, Tang W & Kong L. miR-146a ameliorates liver ischemia/reperfusion injury by suppressing IRAK1 and TRAF6. *PLoS One*. 9 (2014) e101530.

22 Lingappan K. NF-κB in oxidative stress. *Curr opin toxicol*. 7 (2018) 81.

23 Toldo S & Abbate A. The NLRP3 inflammasome in acute myocardial infarction. *Nat Rev Cardiol*. 15 (2018) 203.

24 Bauernfeind FG, Horvath G, Stutz A, Alnemri ES, MacDonald K, Speert D, Fernandes-Alnemri T, Wu J, Monks BG & Fitzgerald KA. NF-κB activating pattern recognition and cytokine receptors license NLRP3 inflammasome activation by regulating NLRP3 expression. *J Immunol*. 183 (2009) 787.